INL/CON-15-37484
PREPRINT

Deuterium retention and blistering in tungsten foils

22nd International Conference on Plasma Surface Interactions in Controlled Fusion Devices

C. N. Taylor, M. Shimada, B. J. Merrill

January 2017

The INL is a
U.S. Department of Energy
National Laboratory
operated by
Battelle Energy Alliance

Deuterium retention and blistering in tungsten foils

C.N. Taylor, M. Shimada, B.J. Merrill

Fusion Safety Program, Idaho National Laboratory, Idaho Falls, ID, USA

To investigate deuterium retention and the onset of blistering, deuterium was implanted in cold rolled tungsten foils at fluences ranging from $3x10^{20}$ to $3x10^{22}$ D/m^2. Ion energies were 300 eV and 2000 eV in order to be below and above the tungsten theoretical damage energy threshold. While energy dependent phenomena were observed, blistering occurs regardless of ion energy. Both plastically and elastically deformed blisters were found, as manifest in before and after micrographs. The fraction of plastically deformed blisters did not saturate at the fluences used in these studies. However, the size of the largest blister that relaxed during TDS does saturate at ~7 μm. A simple conceptual model is presented, which proposes that the deuterium released from elastically deformed blisters appears at ~600 K in the thermal desorption spectra, which is consistent with large vacancy clusters.

Keywords: Tungsten, deuterium, retention, blistering, thermal desorption spectroscopy

Corresponding author: C.N. Taylor, chase.taylor@inl.gov

Highlights:

- Blister formation is more dependent on ion flux than ion energy.
- Elastically deformed blisters release deuterium at ~600 K in thermal desorption spectra.
- The size of the largest blister that relaxes during heating saturates at 6-7 μm.
- The number of plastically deformed blisters increases with ion fluence.

1. Introduction

Hydrogen isotope retention in plasma facing components (PFC) plays a critical role in fusion safety and fuel management. Retention is exacerbated as vacancies and voids are produced in the PFCs due to irradiation damage. Fusion neutrons will produce damage throughout the bulk of materials, thus posing additional concerns for in-vessel tritium inventory. Ion damage from deuterium, tritium, and helium mainly results in near-surface damage, largely dictated by the ion energy as well as flux and fluence. Binary collision approximation (BCA) calculations of the displacement energy threshold,

$$E_{max} = \frac{4M_W M_D}{(M_W + M_D)^2} E_D,$$

where M_W is the mass of tungsten, M_D is the mass of deuterium, and E_D is the energy of the deuterium ion, show that for a minimum displacement energy of 40 eV for tungsten [1], a deuterium ion requires approximately 933 eV/ion to create lattice displacements. However, larger scale damage phenomena occur well below the theoretical damage threshold energy and beyond the ion penetration depth. For example, a layer of nano-tendril tungsten fuzz forms under low energy, high fluence helium irradiation that can grow to be microns in thickness [2]. Similarly, deuterium ions at several hundred eV should have a range of less than 10 nm in tungsten, however blisters form with a 'skin' thickness well beyond the projected range of the ions [3-5]. Precise understanding of the impact that these structures have on deuterium behaviour (e.g. migration, permeation and trapping) remains uncertain.

Tungsten blistering has been investigated under many conditions [6-13]. Few studies have used low flux and fluence to study the onset of blistering and its effect on deuterium retention and the corresponding desorption profile. Deuterium retention in tungsten is investigated at implantation fluences between $3x10^{20}$ and $3x10^{22}$ m^{-2} using thermal desorption spectroscopy (TDS). At these relatively low fluences, we investigate deuterium retention and desorption within the context of blister emergence for cold rolled tungsten foils.

2. Material and methods

Tungsten samples were prepared by punching a 16.5 mm disk from a sheet of 0.05 mm thick, 99.95% pure W foil (Alfa Aesar). Samples were cleaned with acetone, ethanol, and deionized water in an ultrasonic bath (5 min each), followed by heating to 1173 K (0.5 K/s) and holding for 30 minutes for stress relief.

Deuterium was implanted into the tungsten samples using the Neutron Irradiated Material Ion Implantation eXperiment (NIMIIX) at Idaho National Laboratory. NIMIIX is a duoplasmatron type, mass analyzed ion accelerator. Two ion energies were used in these experiments in order to be above and below the minimum damage threshold energy. An ion energy of 2.0 keV/D^+ was achieved by a 6.0 keV/D_3^+ beam, and likewise 0.3 keV/D^+ was obtained from 0.9 keV/D_3^+. At 2.0 keV/D^+ the ion flux was 1.56 ± 0.81 x 10^{19} D/m^2s, and at 0.3 keV/D^+ the average flux was about an order of magnitude less (see Table 1). The samples were irradiated at room temperature, however, ion beam heating caused the sample temperature to increase to no more than 341 K during the 2.0 keV/D^+

irradiations. A 50 μm thick, 3.5 mm diameter tungsten mask was placed over each sample in an attempt to obtain uniform implantation across all samples. The choice of material, and thinness, of the mask reduce the possibility, and impact, of mask-to-sample sputtering contamination.

Table 1. List of samples and ion irradiation conditions.

Sample	Beam	E_{ion} (keV)	Flux (D/m^2s)	Fluence (D/m^2)	T_{max}
WF15_025	D_3^+: 900 eV	0.3	7.3×10^{17}	1.0×10^{21}	299 K
WF15_028	D_3^+: 900 eV	0.3	1.3×10^{18}	3.2×10^{21}	299 K
WF15_029	D_3^+: 900 eV	0.3	1.6×10^{18}	1.0×10^{22}	299 K
WF15_030	D_3^+: 900 eV	0.3	1.7×10^{18}	3.2×10^{22}	299 K
WF15_031	D_3^+: 6000 eV	2.0	2.8×10^{19}	3.2×10^{20}	310 K
WF15_032	D_3^+: 6000 eV	2.0	2.8×10^{19}	5.6×10^{20}	310 K
WF15_021	D_3^+: 6000 eV	2.0	1.6×10^{19}	1.0×10^{21}	~315 K
WF15_027	D_3^+: 6000 eV	2.0	2.8×10^{19}	3.2×10^{21}	~310 K
WF15_024	D_3^+: 6000 eV	2.0	1.2×10^{19}	1.0×10^{22}	317 K
WF15_026	D_3^+: 6000 eV	2.0	2.5×10^{19}	3.2×10^{22}	~310 K

Following ion implantation, scanning electron microscopy (SEM) was performed. Images were taken using backscatter collection mode. Samples were mechanically scratched to provide a fiducial, and polar coordinates were taken so that the same area could be located and imaged after removing/reloading the samples.

Thermal desorption spectroscopy (TDS) was performed 9-12 days after implantation, to quantify D retention in the W samples. It is acknowledged that a delay between implantation and TDS affects retention results, but this effect diminishes after ~100 hours [14]. The TDS system uses an infrared tube furnace to heat samples with a linear ramp rate of 0.5 K/s to a final temperature of 1173 K. Sample temperature was redundantly monitored and controlled with a dual, 1/16" sheathed, grounded, type K, thermocouple that was in physical contact with the sample surface. Desorbed deuterium was measured using a quadrupole mass spectrometer (QMS, MKS eVision+). The TDS system was calibrated for three different leak rates with calibrated deuterium leaks. Background was determined by performing the TDS sequence on a cleaned and stress relieved, but otherwise virgin W sample. After subtracting the background from experimental data, contribution from HD was negligible. SEM images were again taken after TDS.

3. Results and discussion

3.1. Deuterium retention

The desorption spectra for W samples implanted with 2.0 keV/D^+ and 0.3 keV/D^+ to various fluences are shown in Figure 1. A comparison between a) and b) shows

immediate differences. First, the intensity of the peaks is much higher for the higher energy implantation. Several factors contribute to this result.

1. An ion energy of 2 keV/D^+ is well above the binary collision approximation damage threshold energy for tungsten and produces damage that can act as additional trapping sites.
2. The flux for 2.0 keV irradiations in this study was approximately one order of magnitude higher than that for 0.3 keV ions. Total D retention has been shown to be influenced by the flux magnitude, which was suspected to be a result of supersaturation of D within the implantation zone. [15-17].
3. The ion implantation depth increases as ion energy increases. Diffusion beginning deeper within the sample will result in less diffusion to, and reemission from the surface.

The second salient feature of Figure 1 is in the peak shapes. The 1 and $3x10^{22}$ D/m^2 irradiations in (a) show clear shoulders. In addition, the broad peaks for the other spectra can reasonably be deconvoluted into two peaks. These two peaks in these spectra are positioned around 475-500 K and 570-585 K. This corresponds reasonably well to the peaks observed by Alimov, et al., despite a significantly higher fluence of 10^{26} D/m^2 [18]. Very good agreement is also found when compared to the low-energy, low fluence experiments by Bission, et al. [14]. The relationship of these peaks to blister evolution will be discussed in Section 3.3.

Total D retention in the W foils is shown in Figure 2. At a given fluence, total retention is greater by about an order of magnitude for the 2.0 keV implantation than the 0.3 keV implantation. Likewise, retention increases as the fluence increases, with good agreement to previously published data [14,19]. The causes for the higher retention is explained also by the three points mentioned above. The QMS was not sensitive enough to delineate the difference between the first two 0.3 keV data points. However, for all fluences and energies used in these experiments, saturation was not expected, nor observed [20].

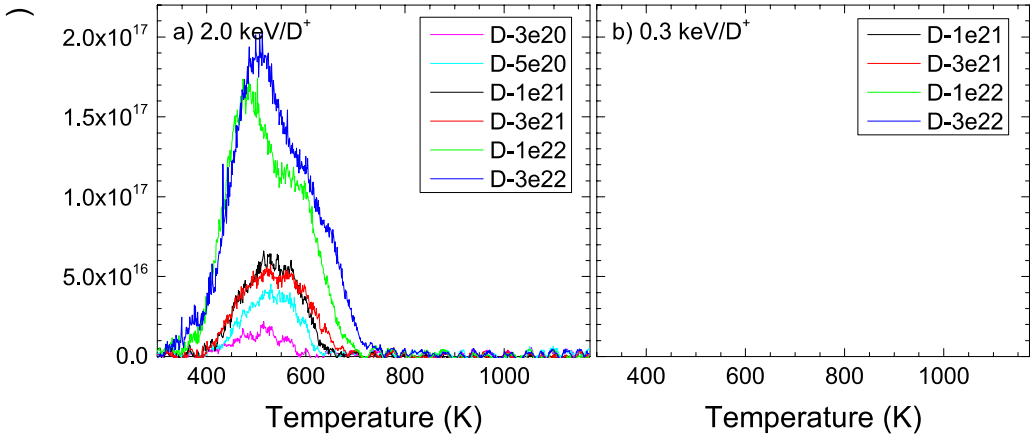

Figure 1. Thermal desorption spectra for a) 2.0 keV/D+ and b) 0.3 keV/D+ implanted into W foils. The fluence (D/m^2) for each sample is shown in the legend.

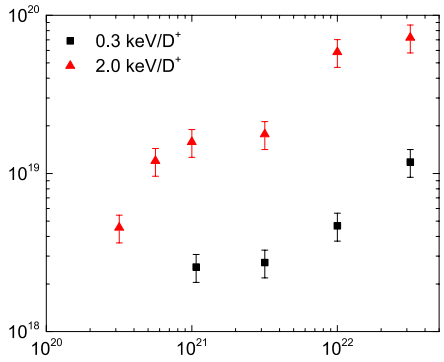

Figure 2. Total retained deuterium versus implanted deuterium for 0.3 keV/D^+ and 2.0 keV/D^+.

3.2. Blistering

In a recent paper, tarnishing of a W sample was observed after a cycle of 0.25 keV/D^+ implantation and TDS was repeated on the same sample tens of times [14]. In the present experiments darkening/tarnishing was also observed on sample surfaces irradiated with 2.0 keV/D^+. These darkened areas, when examined under a microscope were revealed to be blisters. However, no blisters were observed in samples irradiated with 0.3 keV/D^+ until fluences of 1-3x10^{22} D/m^2 (not shown). There is clearly a fluence dependence on blister size and number density even at low ion energies [11].

SEM images were taken of the samples before and after TDS. Care was taken to image the same region before and after TDS, using polar coordinate system from a known landmark, to track the blister alteration. Because this effort focused on conspicuous features for tracking, it is possible that the areas imaged differ from other areas on the sample. Accordingly, no quantification will be made regarding absolute blister size or density. For the 0.3 keV/D^+ samples, blisters were only observed before TDS at ion implantation fluences greater than 1 x 10^{22} D/m^2 before TDS, and after TDS no blisters were observed in any of these samples. Because blisters *were* observed with 0.3 keV/D^+ ions we determine that blistering is more strongly influenced by flux, rather than ion energy. If ion energy were the sole contributing factor, one would not expect to see blisters on any of the 0.3 keV/D^+ samples. Various models proposes that blisters form due to super-saturation of deuterium in the implantation zone due to high flux, which compresses and pushes the deuterium front to deeper layers [3,7,17]. The lateral stress increases as the compressive deuterium layer thickens, until a point is reached when local delamination ensues and a blister forms [3]. In order for super-saturation to occur, the implantation flux must exceed the diffusion rate. This suggests that blister formation is highly flux dependent.

Blistering was very abundant in samples implanted by 2.0 keV/D^+, as shown in Figure 3. The white arrows point to features in both the before and after TDS micrographs intended to provide image orientation. The blister shapes were domed and

on the order of several μm in diameter. Multi-lobed blister clusters were also observed, especially as the D fluence increased, as seen in e).

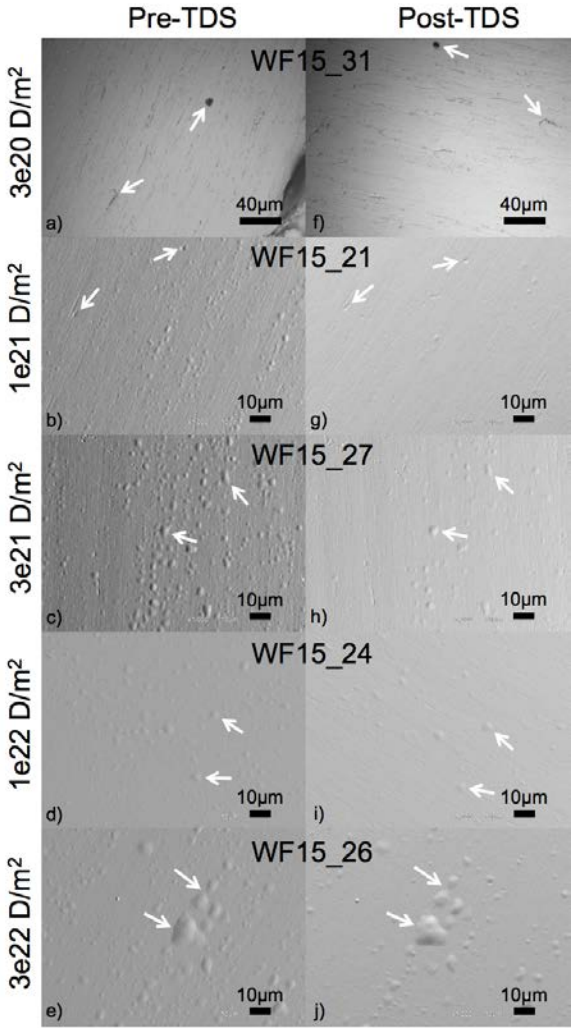

Figure 3. SEM images of W foils before a) – e) and after TDS f) – j) implanted with 2 keV/D^+ after various fluences. Images a) and f) were taken with an optical microscope. White arrows point to orienting features in the before and after micrographs.

After TDS, many blisters remain, as shown in Figure 3 f) – j). It is clear that the number of blisters is significantly less after TDS. Very few blisters were observed in sample WF15_31 before TDS (visible in the top-left corner of pane a) and elsewhere not shown), and no blisters were found anywhere on the sample after TDS. The percentage of blisters that survived TDS (i.e., plastically deformed blisters) for each of the samples is shown in Figure 4 (left-axis). Up to a fluence of $3x10^{22}$ D/m^2 blister survival saturation is not reached, and over 40% of blisters remained after TDS at this fluence. This differs from other studies that showed ~75% of blisters relaxed when heating to approximately the same temperature, 1200 K [7]. The fluence was two orders of magnitude larger than those discussed presently, which according to the trend shown in Figure 4 should result in at least 40% of the blisters remaining after TDS. The ion flux was also an order of

magnitude larger than here. In Section 3.1, the effect of flux on retention was discussed. Here, with regards to blister relaxation, flux is also suspected to play a role. However, if the flux already exceeds the diffusion rate out of the implantation zone, one would expect further increasing the flux to result in larger and an increased number of plastically deformed blisters. Surface preparation, orientation of grain structure, etc., can also affect the outcome of blisters. Further experiments that simultaneously control the flux and fluence are required to elucidate these behaviors.

The size of the largest blister that relaxed during TDS was recorded, and is also shown in Figure 4 (right-axis). Blister relaxation indicates that the blister was only elastically deformed [7]. The blisters that remain after TDS were plastically deformed. The size of the largest blister found to relax after TDS increases as the fluence increases, however in this case a saturation effect is observed. Here, the largest blisters to relax were ellipses that were 6-7 μm in the longest direction. Many blisters also survived that were only 1-2 μm in diameter. Using the present characterization techniques, we could not determine the three-dimensional geometry of blisters. Others have shown that the [111] grain orientation is most prone to blister formation [13,21,22]. Future experiments should explore the 3D structure of the blisters, as well as investigate the saturation of blister relaxation and blisters remaining after TDS.

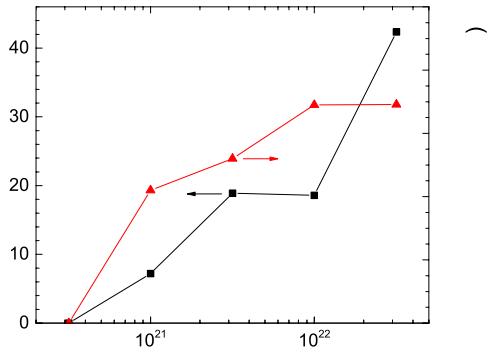

Figure 4. Percentage of blisters remaining after TDS (left axis), and the largest blister eliminated (relaxed) after TDS (right axis). Lines drawn to guide the eye.

3.3. Correlating blisters to TDS spectra

Plastically deformed tungsten is suspect to invoke different deuterium retention mechanisms than virgin, or elastically deformed W. This can be observed in the TDS desorption spectra in Figure 1 a) where, for the highest two fluences, the high temperature peak (570-585 K) decreases relative to the low temperature peak (475-500 K).

A simple conceptual model is presented to correlate blister bursting with the TDS spectra.

1. *Blisters contain high pressure deuterium.*
   Focused ion beam studies probed individual blisters and observed marked deuterium release as the blister was punctured [7].
2. *Blisters burst throughout the heating ramp.*

At very slow heating rates of a few K/min, individual blisters bursts are distinguishable by a properly tuned QMS [8]. At high heating rates or with an improperly tuned QMS, individual blister burst events overlap and appear as a noisy spectrum. In the present experiments, several pronounced spikes, that are well above the noise level, are observed for the 1 and 3 x 10^{23} D/m^2 data curves in Figure 1, which are suspected to be attributed to blister bursts.

3. *Blisters with higher pressure burst more easily (lower temperature).*
   Gas pressure within the blisters can be on the order of a few GPa [3]. Assuming uniform spatial implantation, the gas pressure in each blister will depend on the blister size, which is further dependent on the tungsten microstructural and mechanical properties (skin thickness, grain orientation, grain density, etc.). Under the ideal gas law, which may be applicable under these conditions [21], the pressure increases proportional to temperature. Blisters that start with a higher pressure will exceed the mechanical limits earlier on in the temperature ramp.
4. *Blisters with lower pressure will release deuterium at a higher temperature.*
   Higher temperatures are required to increase the blister gas pressure sufficient to cause a burst event. In the case that a burst event does not occur and deuterium is released via desorption, a release temperature of ~600 K has been associated with desorption from vacancy clusters [23], which corresponds well to the shoulder observed in Figure 1.
5. *The mechanism by which deuterium is released depends on whether the blister is plastically or elastically deformed.*

Shu, et al., reported a variety of formations when blisters burst, including fracturing at grain boundaries and between blister layers, bursting at the side and top of blisters, blisters that burst with partially and fully removed tops, and tails that release deuterium through a tunnel to the nearby free surface [9]. In each case, the blister shell was visible after TDS, indicating plastic deformation. To our knowledge, no cases have been reported where these post-TDS burst mechanisms were observed where the blister shell subsequently relaxed. The only one of these burst mechanisms that intuitively could be compatible with elastically deformed blisters is bursting with a tail. Unfortunately, locating these tails would be quite challenging without an accompanying blister to serve as a landmark. Therefore, we hypothesize that elastically deformed blisters release deuterium via a tail burst event, or through desorption. This conceptual model is presented for the purpose of correlating blister evolution with TDS spectra. It is acknowledged that "regular" desorption methods (i.e., desorption from interstitial sites, vacancies, vacancy clusters, grain boundaries) from blister-free regions still contribute to the desorption spectra. Kolasinski, et al., propose that blisters are responsible for ~28% of deuterium retention in ITER grade tungsten under their given conditions, but point out that blister formation and diffusion in other tungsten grades is significantly different [21].

The samples with a fluence of 3 x $10^{21\text{-}22}$ D/m^2 in Figure 1 show a prominent high-temperature shoulder. The shoulder emerges as the high-temperature component decreases (note: both the high and low temperature peaks increase with fluence; the increase in the low-temperature component is simply stronger). This decrease corresponds to a decrease in the fraction of elastically deformed blisters (see Figure 4). Considering the conceptual model above, we therefore propose that deuterium desorption from elastically deformed blisters primarily occurs at higher temperatures.

4. Conclusions

Low deuterium flux and fluence ion beams were used to investigate and correlate tungsten blistering to deuterium retention. We found indications that ion flux had a greater influence on blister formation than ion energy, and heating to 1173 K caused relaxation of some of the elastically deformed blisters. More blisters formed at 2 keV than 0.3 keV, but this was attributed to the higher ion flux that resulted at this energy. The fraction of plastically deformed blisters increased as the ion fluence increased, and up to a fluence of 3×10^{22} D/m^2, no saturation of this effect was observed. However, the size of the largest blister that relaxed did reach a threshold value of 6-7 μm, suggesting that blisters larger than 7 μm will rarely be elastically formed. During thermal desorption spectroscopy, retention was found to increase as ion flux, fluence, and energy increase. Two peaks were observed in the ranges of 475-500 K and 570-585 K. Release of deuterium from elastically deformed blisters was primarily attributed to the high temperature peak, which is consistent with large vacancy clusters.

Acknowledgements

This work was prepared for the US Department of Energy, Office of Fusion Energy Sciences, under the DOE Idaho Field Office contract number DE-AC07–05ID14517.

References

[1] Standard Practice for Neutron Radiation Damage Simulation by Charged-Particle Irradiation, 2009 ed., ASTM International, West Conshohocken, PA, 2009.
[2] M.J. Baldwin, R.P. doerner, Journal of Nuclear Materials 404 (2010) 165–173.
[3] N. Enomoto, S. Muto, T. Tanabe, J.W. Davis, A.A. Haasz, Journal of Nuclear Materials 385 (2009) 606–614.
[4] T. Tanabe, Physica Scripta T159 (2014) 014044.
[5] S. Lindig, M. Balden, V.K. Alimov, T. Yamanishi, Physica Scripta T138 (2009) 014040.
[6] H.Y. Xu, W. Liu, G.N. Luo, Y. Yuan, Y.Z. Jia, B.Q. Fu, G. De Temmerman, Journal of Nuclear Materials 471 (2016) 51–58.
[7] M. Balden, S. Lindig, A. Manhard, J.-H. You, Journal of Nuclear Materials 414 (2011) 69–72.
[8] A. Manhard, U. von Toussaint, T. Dürbeck, K. Schmid, W. Jacob, Physica Scripta T145 (2011) 014038.
[9] W.M. Shu, E. Wakai, T. Yamanishi, Nuclear Fusion 47 (2007) 201–209.
[10] K. Tokunaga, M.J. Baldwin, R.P. doerner, N. Noda, Y. Kubota, N. Yoshida, T. sogabe, T. Kato, B. Schedler, Journal of Nuclear Materials 337-339 (2005) 887–891.
[11] W. Wang, J. Roth, S. Lindig, C.H. Wu, Journal of Nuclear Materials 299 (2001) 124–131.
[12] M.Y. Ye, H. Kanehara, S. Fukuta, N. Ohno, S. Takamura, Journal of Nuclear Materials 313 (2003) 72–76.
[13] W.M. Shu, A. Kawasuso, Y. Miwa, E. Wakai, G.N. Luo, T. Yamanishi, Physica Scripta T128 (2007) 96–99.
[14] R. Bisson, S. Markelj, O. Mourey, F. Ghiorghiu, K. Achkasov, J.M. Layet, P. Roubin, G. Cartry, C. Grisolia, T. Angot, Journal of Nuclear Materials 467 (2015) 432–438.
[15] M. Poon, R.G. Macaulay-Newcombe, J.W. Davis, A.A. Haasz, Journal of Nuclear Materials 307-311 (2002) 723–728.
[16] O.V. Ogorodnikova, J. Roth, M. Mayer, Journal of Applied Physics 103 (2008) 034902–034902.
[17] V.K. Alimov, W.M. Shu, J. Roth, S. Lindig, M. Balden, Journal of Nuclear Materials 417 (2011) 572–575.
[18] V.K. Alimov, B. Tyburska-Püschel, S. Lindig, Journal of Nuclear Materials 420 (2012) 519–524.
[19] Z. Tian, J.W. Davis, A.A. Haasz, Journal of Nuclear Materials 399 (2010) 101–107.
[20] A.A. Haasz, J.W. Davis, M. Poon, R.G. Macaulay-Newcombe, Journal of Nuclear Materials 258 (1998) 889–895.
[21] R.D. Kolasinski, M. Shimada, Y. Oya, D.A. Buchenauer, T. Chikada, D.F. Cowgill, D.C. Donovan, R.W. Friddle, K. Michibayashi, M. Sato, Journal of Applied Physics 118 (2015) 073301.

[22] Y.Z. Jia, W. Liu, B. Xu, G.N. Luo, S.L. Qu, T.W. Morgan, G. De Temmerman, Journal of Nuclear Materials 477 (2016) 165–171.
[23] O.V. Ogorodnikova, T. Schwarz-Selinger, K. Sugiyama, V.K. Alimov, Journal of Applied Physics 109 (2011) 013309.